

Numerical Approach to Determine the Simultaneous Influence of Thermal Radiation and Chemical Reaction Over MHD Stagnation-Point Flow of Sisko Nanofluid

A.A. HUSSAINI¹, ISAH ABDULLAHI², ADAMU ABDULKADIR TATA³, ALI MUSA⁴

^{1,2} Department of Mathematical Sciences, Abubakar Tafawa Balewa University, Bauchi, Nigeria.

³ Department of Mathematics and Statistics, Federal Polytechnic Bauchi, Bauchi, Nigeria

⁴ Department of Mathematics and Statistics, Yobe State University, Damaturu, Nigeria.

Abstract- In this research a numerical investigation is performed to show the effects of thermal radiation and chemical reaction on the hydro magnetic stagnation-point flow of Sisko nanofluid over a linearly stretching sheet by considering viscous dissipation and Joule heating with suction/injection. A suitable set of similarity transformations is considered in order to convert the basic partial differential equations into a set of coupled nonlinear ordinary differential equations. An efficient numerical method along with shooting technique is involved in order to solve the reduced governing basic equations. The influences of several emerging physical parameters of Sisko nanofluid on the profiles of velocity, temperature, solutal concentration, nanoparticle volume fraction, skin friction coefficient, Nusselt number, and Sherwood number have been studied and analyzed in detail through graphs and tables. It is found that the skin friction coefficient decays more rapidly against the material parameter of Sisko fluid. Also, it is noticed that the Brownian motion and thermophoresis parameter have the reverse effects on Sisko nanofluid Sherwood number. It is analyzed that the Nusselt number decreases with an increase in the values of thermophoresis parameter, Brownian motion parameter, and Eckert number, while its value increases with material parameter and DuFour solutal Lewis number. It is observed that the Sherwood number has ascending behavior for thermophoresis and, Brownian motion parameters, whereas nanofluid Sherwood number gets amplified with a hike in the Nano Lewis number parameter for all the values of Brownian motion parameter.

I. INTRODUCTION

The studies on heat and mass transfer with the non-Newtonian fluid have taken a vital role in the modern technology and industrial applications, such as heat exchangers, petroleum reservoirs, material process system, molten plastic products, wall paint, food products, lubricant oil, greases, etc. Various mathematical models were developed in the past to explain the characteristics of the non-Newtonian fluids, but those may not alone describe all the capabilities of the non-Newtonian fluids present in nature. To overcome some of the limitations: Sisko et al. 1958 introduced a three-parameter Sisko fluid model, with which we can examine the cases of shear-thinning and shear-thickening characteristics of the fluid. Nanofluid was first employed by Choi 1955 and is proficient in various industrial applications, such as it can be used as a coolant in nuclear reactors and hybrid-powered engines, microchips in computers, and mostly used in the field of current nanotechnologies. Other related researchers are Macha et al. 2017, Eid et al. 2008, Mahny et al. 2018 and Jawad et al. 2019, It has been found from previous studies that nanofluids can retain micro/millimeter-sized particles with dimensions smaller than 100 nm. Moreover, it may contain various types of nanoparticle like metallic, nonmetallic, oxides, CNTs (carbon nanotubes) or carbides, etc. With different base fluids like ethylene glycol, water, engine oil, etc. The addition of nanoparticles in the base fluids can boost up the thermal conductivities of the functioning fluids. The two important mechanisms of the nanoparticles are the Brownian and thermophoresis behavior.

Among several non-Newtonian models, Sisko fluid model showed awesome achievements due to its huge

applications in the chemical and metallurgical processing industry. Also, the importance of Sisko model has grown up because it can predict the properties of numerous non-Newtonian fluids. This model is a three-parametric model which can be assumed as a generic of power-law and Newtonian model.

The study of magnetic nanofluid flow and heat transfer is applicable in the polymer industry, and metallurgy. The physical characteristic of such fluid has been judged by the following previous researchers by making changes in the strength of the magnetic field: Awais et al, 2017, Hayat et al. 2018, Daniel et al. 2019, Ali et al, 2020.

Furthermore, Brownian force plays an important role when the temperature of the conventional fluid is much higher. In the case when the nanoparticles in base fluid has a constant temperature gradient then thermophoresis is considered as a crucial impact of the Brownian motion. For the existence of temperature gradient in the flow region of the suspension, small particles disperse faster in the hotter domain and slower in the colder domain. The consequence of nanoparticle dispersion from higher temperature region to a cooler region of the fluid domain is known as thermophoresis. This has been investigated by some other researchers: Prasannakumara et al. 2017, Soomro et al, 2018 and Pal and Mandal, 2019.

Another important factor which affects the heat transfers characteristics of the fluid flow is the Joule heating. The fluid flow with Joule heating has extensive applications in an electric device. In recent years, the engineers and scientists are avidly interested to increase the total efficiency of various mechanical systems and industrial machinery. These types of difficulties can be handled by decreasing the temperature produced due to Ohmic dissipation or Joule heating. Khan et al. 2019 presented Sisko thin fluid flow and heat transfer over an unsteady stretching sheet with a constant magnetic field and thermal radiation. A numerical study was performed by Sharma and Bisht 2019 to study the effect of Joule heating on heat transfer of electrically conducting Sisko nanofluid past a stretching sheet with convective boundary conditions. Ijaz et al. 2010 investigated the nonlinear convective flow of a Sisko nanofluid due to

a stretchable rotating disk with nonlinear thermal radiation and non-uniform heat generation/absorption. They also considered the effects of Joule heating and viscous dissipation.

Which brings the research to my base paper titled: heat and mass transfer of Magnetohydrodynamic Sisko nanofluid flow over a stretching sheet with combined effects of Joule heating and viscous dissipation with suction/injection by Pal and Mandal 2020. Hence, the main motivation of present analysis is to study the effect (influence) of thermal radiation and chemical reactions simultaneously on this model.

II. PROBLEM FORMULATION

We consider two-dimensional stagnation point flow of an incompressible magnetohydrodynamic (MHD) Sisko nanofluid over a stretching sheet having linear velocity $u_w(x) = cx$ and velocity of the free stream flow is $u_\infty = dx$, where c, d are constants, x is the coordinate measured along with the stretching sheet. The sheet is kept at a constant temperature T_w , solutal concentration C_w , and nanoparticle concentration ϕ_w . A distance far away from the stretching sheet, temperature, solutal concentration, and nanoparticle volume fraction are denoted by T_∞ , C_∞ , and ϕ_∞ , respectively. Thermophoresis and Brownian motion effects are taken into account. The magnetic field of strength B_0 is applied in the transverse direction to the flow. Also, the effect of Joule heating is considered here. The magnetic Reynolds number is taken to be small and thus the induced magnetic field is neglected. Nanoparticles in the base fluid are assumed to be in thermal equilibrium and no slip exists at the stretching sheet. The flow takes place at $y \geq 0$, where y is the coordinate measured normal to the stretching sheet (see Figure 1) below.

Here u and v are the velocity components along the x and y -directions, respectively; ρ_f is the density of the base fluid, ρ_s is the reference density of the solid fraction, μ_f is the viscosity of the fluid fraction, a and b are the material constants of the Sisko fluid, n ($n > 0$) is a power-law index, ν is the kinematic viscosity of the fluid, σ is the electrical conductivity, B_0 is the

magnetic field flux density, α_m is the thermal conductivity, D_B is the Brownian motion diffusion coefficient, D_T is the thermophoresis diffusion coefficient, D_{TC} and D_{CT} are Soret and Dufour diffusivities, D_S is the solutal diffusivity, $\tau = (\rho C)_p / (\rho C)_f$ is the ratio of the effective heat capacity of the nanoparticles and heat capacity of the fluid, T is the fluid temperature, C the solutal concentration, ϕ is the nanoparticle volume fraction, respectively.

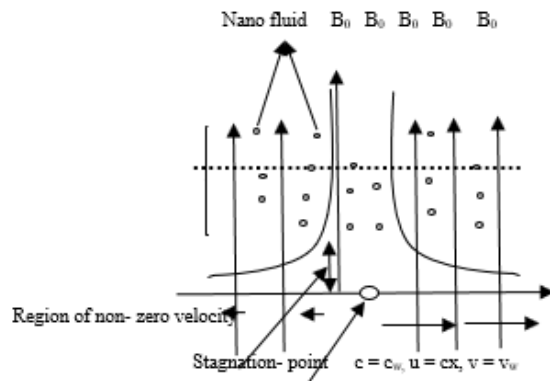


Figure 1: physical model

These are the governing equations for the conservation of Mass, Momentum, Energy, Mass Transfer Diffusion and Nanoparticles volume fraction after the modifications just as in Pal and Mangal (2020):

$$\begin{aligned} \frac{\partial u}{\partial x} + \frac{\partial v}{\partial y} &= 0 \quad (1) \\ u \frac{\partial u}{\partial x} + v \frac{\partial u}{\partial y} &= u_{\infty} \frac{du_{\infty}}{dx} + \frac{a}{\rho f} \left(\frac{\partial^2 u}{\partial y^2} \right) \\ &- \frac{b}{\rho f} \frac{\partial}{\partial y} \left[\left(-\frac{\partial u}{\partial y} \right)^n \right] + \frac{\sigma B_0^2}{\rho f} (u_{\infty} - u) \quad (2) \end{aligned}$$

$$\begin{aligned} u \frac{\partial T}{\partial x} + v \frac{\partial T}{\partial y} &= \alpha_m \left(\frac{\partial^2 T}{\partial y^2} \right) + \frac{\sigma B_0^2}{(\rho C_p) f} (u_{\infty} - u)^2 \\ &+ \frac{1}{(\rho C_p) f} \left\{ a \left(\frac{\partial u}{\partial y} \right)^2 + b \left[\left(-\frac{\partial u}{\partial y} \right)^{n+1} \right] \right\} \\ &+ \tau \left\{ D_B \left(\frac{\partial \phi}{\partial y} \frac{\partial T}{\partial y} \right) + \frac{D_T}{T_{\infty}} \left[\left(\frac{\partial T}{\partial y} \right)^2 \right] \right. \\ &\left. + D_{TC} \left(\frac{\partial^2 C}{\partial y^2} \right) \right\} \\ &+ \left[-\frac{1}{(\rho C_p) f} \frac{\partial q_r}{\partial y} \right] \quad (3) \end{aligned}$$

$$u \frac{\partial C}{\partial x} + v \frac{\partial C}{\partial y} = D_S \left(\frac{\partial^2 C}{\partial y^2} \right) + D_{CT} \left(\frac{\partial^2 T}{\partial y^2} \right) - K_1 (C - C_{\infty}) \quad (4)$$

$$u \frac{\partial \phi}{\partial x} + v \frac{\partial \phi}{\partial y} = D_B \left(\frac{\partial^2 \phi}{\partial y^2} \right) + \frac{D_T}{T_{\infty}} \left(\frac{\partial^2 T}{\partial y^2} \right) \quad (5)$$

Together with the following boundary conditions;

$$\begin{aligned} \text{At } y &= 0: \\ u &= u_w = cx, v = v_w, T = T_w, C = C_w, \phi = \phi_w \quad (6) \end{aligned}$$

$$\begin{aligned} \text{As } y &\rightarrow \infty: \\ u &= u_{\infty} = dx, v \rightarrow 0, T \rightarrow T_{\infty}, C \rightarrow C_{\infty}, \phi \rightarrow \phi_{\infty} \quad (7) \end{aligned}$$

As well as the non-Dimensional Quantities which are as follows:

$$\begin{aligned} U &= cx f'(\eta) \\ v &= C \left(\frac{C^{n-2}}{\rho f / b} \right)^{\frac{1}{n+1}} \left(\frac{2n}{n+1} F(\eta) + \frac{1-n}{1+n} \eta F'(\eta) \right) x^{\frac{n-1}{n+1}} \\ \theta(\eta) &= \frac{T - T_{\infty}}{T_w - T_{\infty}}, \quad \Rightarrow \quad T = \theta T_w \\ S(\eta) &= \frac{C - C_{\infty}}{C_w - C_{\infty}} \quad \Rightarrow \quad C = S C_w \\ \Phi(\eta) &= \frac{\phi - \phi_{\infty}}{\phi_w - \phi_{\infty}} \quad \Rightarrow \quad \phi = \Phi \phi_w \\ \eta &= y \left(\frac{C^{2-n}}{b / \rho f} \right)^{\frac{1}{n+1}} x^{\frac{1-n}{1+n}} \quad (8) \end{aligned}$$

After substituting equation 6,7 and 8 into equations 1-5, equation 1 is identically satisfied by the stream

function: $u = \frac{\partial \psi}{\partial y}$, $v = -\frac{\partial \psi}{\partial x}$, and we obtained the

following ordinary differential equations

$$A F''' + n (-F'')^{n-1} F''' + \frac{2n}{n+1} F F'' + \frac{d^2}{c^2} - F'^2 + M \left(\frac{d}{c} - F' \right) = 0 \quad (9)$$

$$\theta'' + \text{Pr} \frac{2n}{n+1} F \theta' + \text{PrMEc}(1-F')^2 + \text{PrEc}[A(F'')^2 + (-F'')^{n+1}] + \text{PrNb} \phi' \theta' + \text{PrNt} \theta'^2 + \text{Nd} S''$$

$$+ \left(\frac{1}{\text{Pr}} + \frac{3}{3} N \right) = 0 \quad (10)$$

$$S'' + \text{LePr} \frac{2n}{n+1} F S' + \text{Ld} \theta'' = 0 \quad (11)$$

$$\phi'' + \text{LePr} \frac{2n}{n+1} F \phi' + \frac{\text{Nt}}{\text{Nb}} \theta'' - \lambda S \quad (12)$$

subject to the following boundary conditions
 $f = \lambda, f'(0) = 1, \theta(0) = 1, S(0) = 1, \phi(0) = 1$ (13).

$$f'(\infty) \rightarrow \frac{d}{c}, \theta(\infty) \rightarrow 0, S(\infty) \rightarrow 0, \phi(\infty) \rightarrow 0 \quad (14).$$

where primes denote the differentiation with respect to η , f' is the dimensionless velocity, T is the dimensionless temperature, S is dimensionless solutal concentration and ϕ is the dimensionless nanoparticle volume fraction of the fluid.

The parameters appeared in Eqs. (9) to (14) are the material parameter of the Sisko fluid A , magnetic parameter or Joule heating parameter M , Prandtl number Pr , Brownian motion parameter Nb , thermophoresis parameter Nt , Lewis number Le , nano Lewis number Ln , modified Dufour parameter Nd , Dufour solutal Lewis number Ld , suction/injection parameter s , N the radiation parameter and Eckert number Ec are defined as:

$$A = \frac{\text{Re}_b^{2/(n+1)}}{\text{Re}_a}, M = \frac{\sigma B_0^2}{\rho_f C}, \text{Pr} = \frac{x u_w \text{Re}_b^{-2/(n+1)}}{c \alpha_m},$$

$$\text{Nb} = \frac{(\rho c)_p D_B (C_w - C_\infty)}{\alpha_m (\rho c)_f}, \text{Nd} = \frac{D_{TC} (C_w - C_\infty)}{\alpha_m (T_w - T_\infty)},$$

$$\text{Le} = \frac{\alpha_m}{D_s}, \text{Ln} = \frac{\alpha_m}{D_B}, \text{Nd} = \frac{D_{TC} (C_w - C_\infty)}{\alpha_m (T_w - T_\infty)},$$

$$\text{Ld} = \frac{D_{CT} (T_w - T_\infty)}{D_s (C_w - C_\infty)}, s = \frac{n+1}{2n} \frac{v_m}{\left(\frac{c^{n+1}}{\rho_f / b} \right)^{1/(n+1)}},$$

$$\text{Ec} = \frac{u_w^2}{C_p (T_w - T_\infty)}. \quad (15)$$

The parameters of engineering interest in heat and mass transport problems are skin-friction coefficient C_{fx} , local Nusselt number Nu_x , Sherwood number Sh_x and nanofluid Sherwood number $\text{Sh}_{x,n}$, which are defined by

$$C_{fx} = \frac{\left(a + b \left| \frac{\partial u}{\partial y} \right| \right)^{n-1}}{\frac{1}{2} \rho_f u_w^2} \left(\frac{\partial u}{\partial y} \right)_{y=0}, \text{Nu}_x = \frac{x \left(\frac{\partial u}{\partial y} \right)_{y=0}}{(T_w - T_\infty)},$$

$$\text{Sh}_x = \frac{-x \left(\frac{\partial C}{\partial y} \right)_{y=0}}{(C_w - C_\infty)}, \text{Sh}_{x,n} = \frac{-x \left(\frac{\partial \Phi}{\partial y} \right)_{y=0}}{(\Phi_w - \Phi_\infty)} \quad (16).$$

Using Eq. (8) in Eq. (16) skin-friction coefficient, local Nusselt number, Sherwood number, and nanofluid Sherwood number can be expressed as:

$$\text{Re}_b^{n+1} C_{fx} = A f''(0) - (-f''(0))'',$$

$$\text{Re}_b^{n+1} \text{Nu}_x = -\theta'(0),$$

$$\text{Re}_b^{n+1} \text{Sh}_x = -S'(0), \text{Re}_b^{n+1} \text{Sh}_{x,n} = -\Phi'(0), \quad (17).$$

where $\text{Re}_a = x u_w \rho_f / a$ and $\text{Re}_b = x^n (u_w)^{n-2} \rho_f / b$ are the local Reynolds numbers.

Reduced form of the skin-friction coefficient, Nusselt number, Sherwood and nanofluid Sherwood number is given by Pal Mandel (2020):

$$C_{fx} = \text{Re}_b^{n+1} C_{fx}, \text{Nu}_r = \text{Re}_b^{n+1} \text{Nu}_x,$$

$$\text{Sh}_x = \text{Re}_b^{n+1} \text{Sh}_x, \text{Sh}_m = \text{Re}_b^{n+1} \text{Sh}_{x,n} \quad (18)$$

III. RESULTS AND DISCUSSION

In this section, the influence of important parameters on the velocity, temperature, solute, and nanoparticle

concentration profiles over a linear stretching sheet is presented by using graphs and tables. Figures1- 15 are drawn to establish the importance of these parameters. Effect of suction thermal conductivity parameter k on the nanoparticle concentration, temperature and velocity profiles are shown in Figures1 to 3 respectively. Since k predicts the behavior of suction of fluid at the surface of sheet that depends upon the positive values of k . It is found that the velocity of fluid, temperature, and nanoparticle concentration all decreases near the boundary wall. In the case of suction, the heated fluid is pushed towards the wall where the buoyancy forces can act to enhance the nanofluid due to the high influence of the viscosity. This effect acts to decrease the wall shear stress, decreases the thermal, and reduces the concentration boundary layer thickness in case of suction.

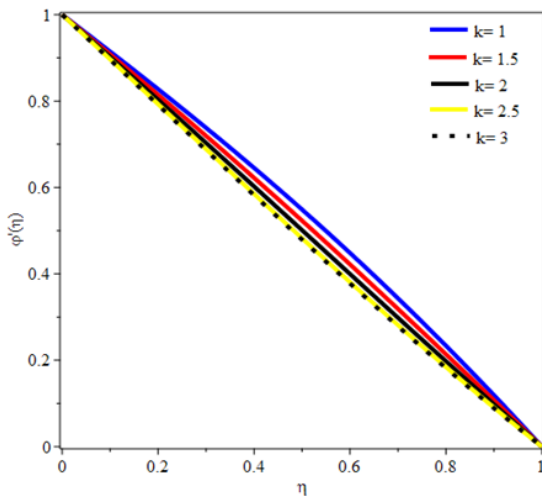


Figure1: effects of thermal conductivity parameter (k) on the nanoparticle concentration profile.

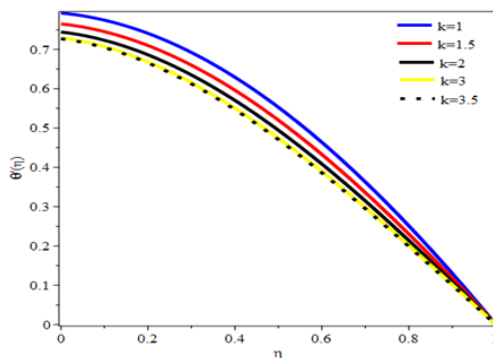


Figure2: effects of thermal conductivity parameter (k) on the temperature profile.

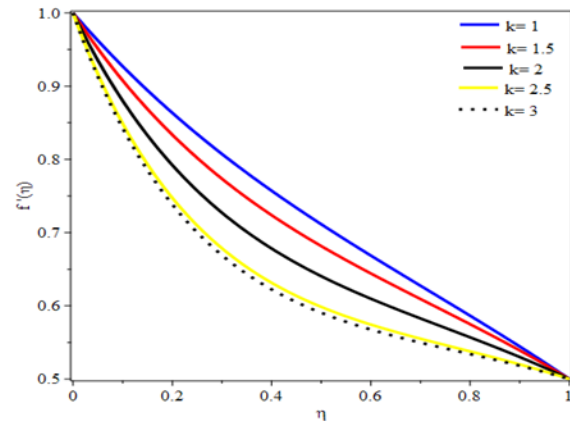


figure3: effects of thermal conductivity (k) parameter on the velocity profile.

As can be observed on the figures 4 to 6 that depicted the effects of Magnetic parameter M on the profiles of velocity, temperature as well as the nanoparticle concentration. The momentum rises with an increase in the values of M , whereas, in both cases of temperature and concentration, increase in the value of magnetic parameter produces decreases in both the profiles.

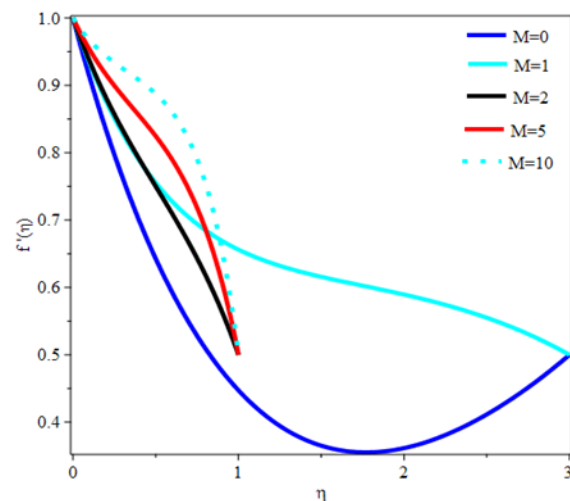


figure4: effects of Magnetic parameter (M) on the velocity profile.

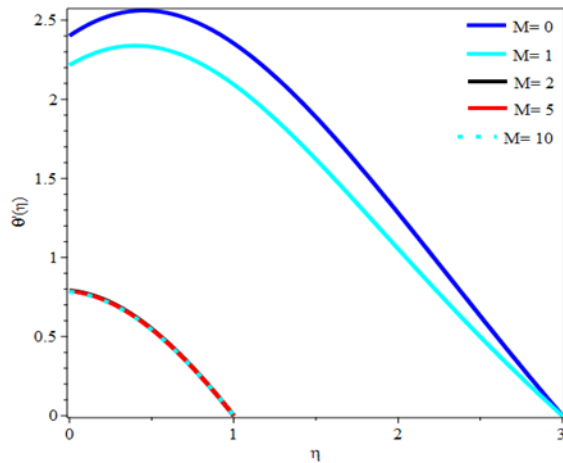


figure5: effects of Magnetic parameter (M) on the temperature profile.

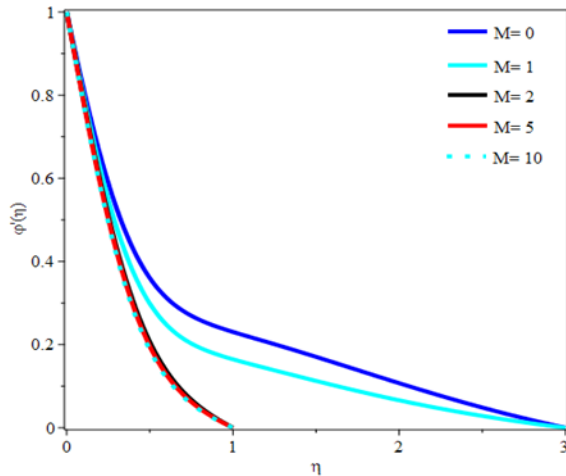


figure6: effects of Magnetic parameter (M) to the nanoparticle concentration profile.

It can be observed from *figure7* and *figure8*, the dual effects of radiation parameter (N) on the temperature profile and nanoparticle concentration profile respectively. In both cases we detected that for any increment in the values of N, it produces increment in both the temperature and concentration profiles. *Figure9* shows the nature of the nanoparticle concentration for ascending values of Lewis number. In this case we detect that the nanoparticle concentration of the fluid decreases drastically with the increase in the values of Lewis number. Furthermore, *figures10* and *11* are plotted in order to see the influence of thermophoresis parameter on the profiles of temperature and nanoparticle concentration

profiles. It can be concluded that increment in the values of thermophoresis parameter (Nt) produces increment in both temperature profile and nanoparticle concentration profile. Due to the thermophoresis phenomenon, a convective flow is formed which causes hot fluid molecules to move from a warm region to cold areas and results increase in temperature along through its path in the surface. Physically, the higher value of Nt is related to the greater mass flux that increases the concentration profile significantly.

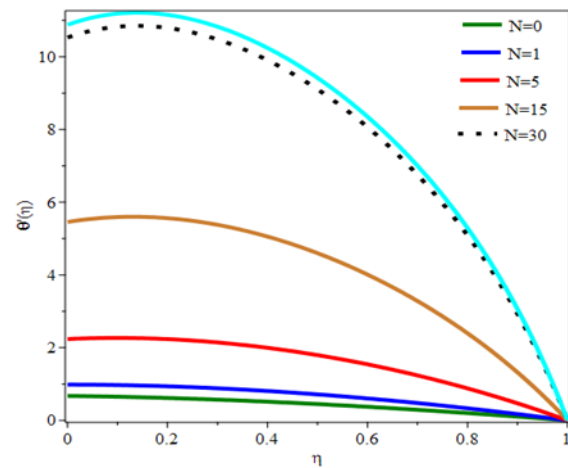


Figure7: effects of radiation parameter (N) on the temperature profile.

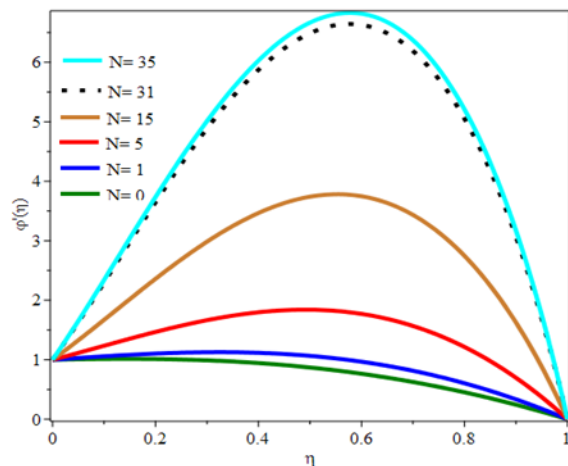


Figure8: effects of radiation parameter (N) on the nanoparticle concentration profile.

Figure12 illustrates the simultaneous effects of chemical reaction parameter together with radiation parameter, in which for any negative values of

chemical reaction, increase in the values of radiation parameter produces increment in the temperature, while for any positive values of chemical reaction parameter, increase in the values of radiation parameter brings about decrease in the temperature profile.

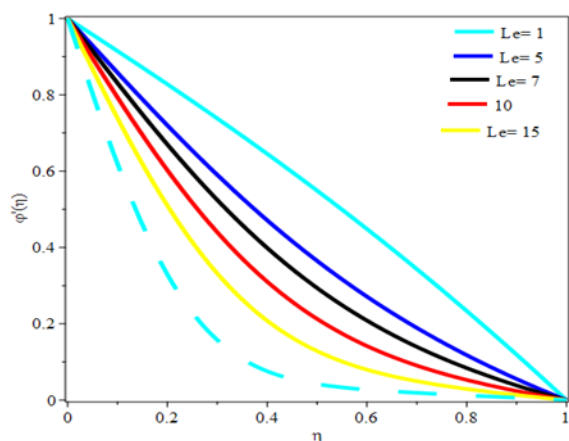


Figure9: effects of Lewis number (Le) on the nanoparticle concentration profile.

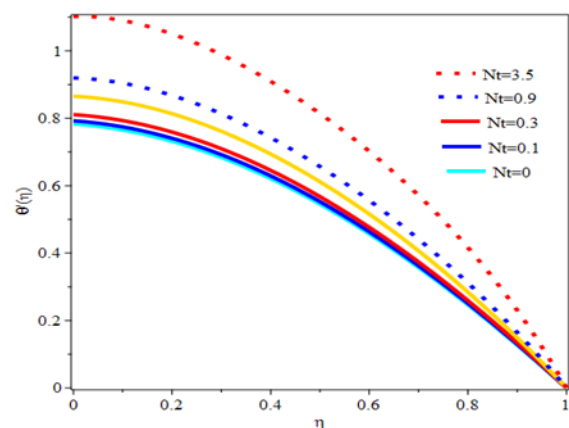


Figure10: effects of thermophoresis parameter (Nt) on the temperature profile.

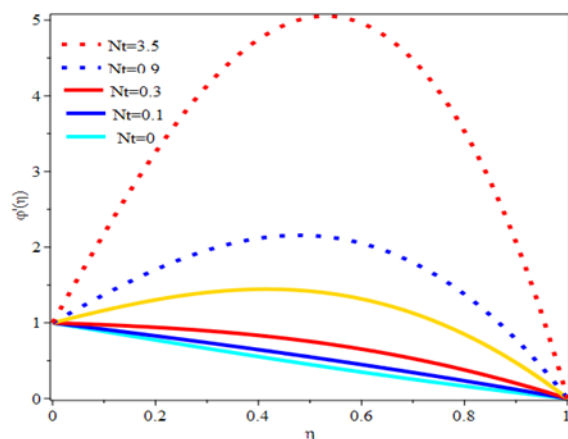


Figure11: effects on thermophoresis parameter (Nt) on the nanoparticle concentration profile.

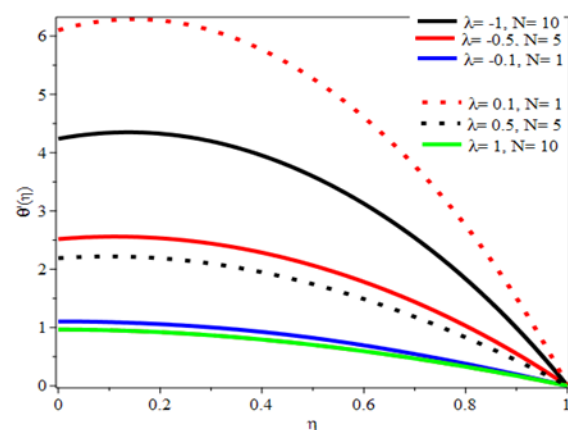


Figure12: effects of chemical reaction parameter (λ) and the radiation parameter (N) on the temperature profile.

It is seen on *figure13* that the nanoparticle concentration is slightly enhanced for any increase in the values of radiation parameter when the chemical reaction have negative values, whereas, the opposite trend is observed for any increment in the values of radiation parameter when the chemical reaction parameter have positive values.

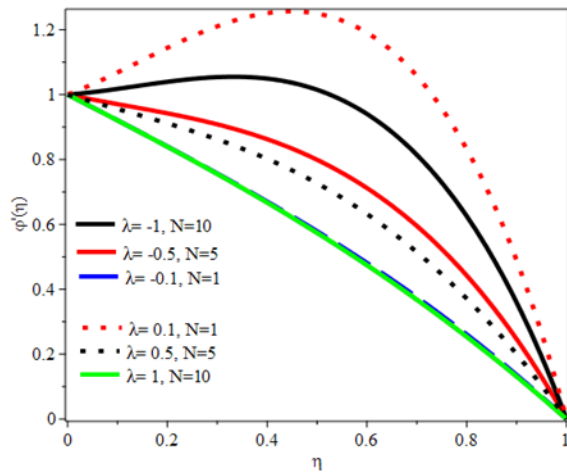


Figure13: effects of chemical reaction parameter (λ) and radiation parameter (N) on the nanoparticle concentration.

Figure14 and figure15 are drawn to establish the importance of Prandtl number on the Nusselt number as well as Sherwood number. We detect that both the Nusselt number and Sherwood number profiles decreases with the increase of the values of Prandtl number.

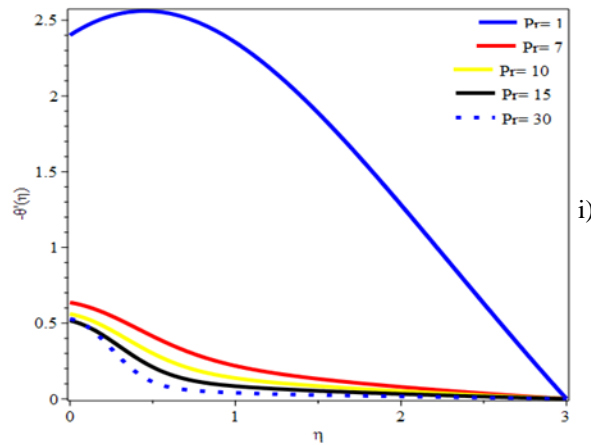


Figure14: effects of Prandtl number on Nusselt number profile.

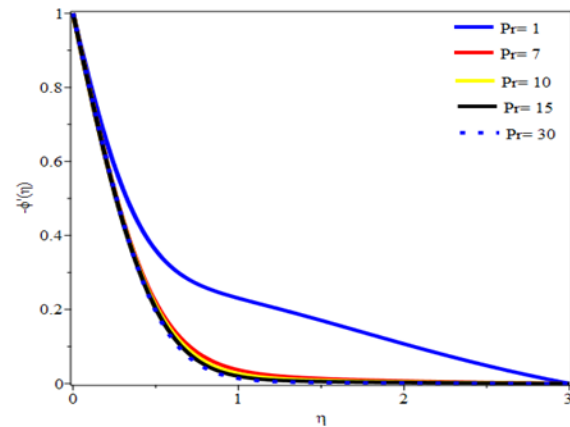


Figure15: effects of Prandtl number on Sherwood number profile.

CONCLUSION

In this investigation we have successfully shown numerically as well as physically the simultaneous effects of thermal radiation and chemical reaction on magnetohydrodynamic (MHD) stagnation- point flow of Sisko nanofluid over a linearly stretching sheet considering viscous dissipation and Joule heating with suction/injection using the Runge- Kutta- Fehlberge method. In this work we have investigated the effects of Sisko fluid material parameter, magnetic parameter, Prandtl number, Brownian motion, thermophoresis, Lewis number, Eckert number, Dufour solutal Lewis number, on the velocity, temperature, nanoparticle concentration, Nusselt number and Sherwood number. At last, these are the possible conclusions we have drawn from the numerical results:

- i. The velocity profile is enhanced with the higher values of thermal radiation parameter (k) and magnetic parameter (M).
- ii. The temperature profile is lowered with the higher values of thermal radiation parameter (k) and the magnetic parameter (M).
- iii. The temperature profile is enhanced with the higher values of radiation parameter (N) and the thermophoresis parameter (N_t).
- iv. As for the positive values of chemical reaction parameter (λ), the temperature profile is decreased for any increment in the values of radiation parameter (N).
- v. As for the negative values of chemical reaction parameter (λ), the temperature profile is increased

- for any increment in the values of radiation parameter (N).
- vi. The nanoparticle concentration is decreased with an increment in the values of chemical reaction parameter (k), magnetic parameter (M) and Lewis number (Le).
 - vii. In both cases of Nusselt number and Sherwood number, a drastic decrease is observed with an increase in the values of Prandtl number (Pr).
 - viii. For the negative values of chemical reaction parameter (k), there is an increase in nanoparticle concentration whenever there is an increase in the radiation parameter (N). On the other hand, the reverse is the case for positive values of chemical reaction parameter.

REFERENCES

- [1] A. G. Madaki, R. Roslan, M. Mohamad, M.G. Kamardan (2016). Analytical Solution of Squeezing Unsteady Nanofluid Flow in the Presence of Thermal Radiation: *J. of Comput. Sci. & Comput. Maths*, 6 (4)
- [2] A. A. Hussaini, A.G. Madaki, A.M. Kwami (2021). "Modified Mathematical Model on the Study of Convective MHD Nanofluid flow with Heat Generation/Absorption"- *Int. J. of Engineering research and technology*, 10 (09) :155- 163.
- [3] A.G. Madaki, R. Roslan, M.S. Rusiman, C.S.K. Raju (2018). "Analytical and numerical solutions of squeezing unsteady Cu and TiO₂-nanofluid flow in the presence of thermal radiation and heat generation/absorption": *Alexandria Engineering Journal*, 57, 1033-1040
- [4] A.S. Khan, Y. Nie, Z. Shah (2019). Impact of thermal radiation on magnetohydrodynamic unsteady thin film flow of Sisko fluid over a stretching surface *Processes* 7 (6) 369
- [5] A.W. Sisko (1958). The flow of lubricating greases, *Ind. Eng. Chem. Res.* 50 (12) 1789e1792.
- [6] B.C. Prasannakumara, B.J. Gireesha, M.R. Krishnamurthy, K.G. Kumar (2017). MHD flow and nonlinear radiative heat transfers of Sisko nanofluid over a nonlinear stretching sheet, *Inform. Med. Unlocked* 9 123 -132.
- [7] Dulal Pal, Gopinath Mandal (2020). Magnetohydrodynamic stagnation-point flow of Sisko nanofluid over a stretching sheet with suction, *Propuls. Power Res.* 9(4): 151- 158
- [8] D. Pal, G. Mandal, K. Vajravalu (2019). Magnetohydrodynamic nonlinear thermal radiative heat transfer of nanofluids over a flat plate in a porous medium in existence of variable thermal conductivity and chemical reaction, *Int. J. Ambient Energy* 1- 30
- [9] F. Hady, F. Ibrahim, H. El-Hawary and A. Abdelhady (2012). *Effect of Suction/Injection on Natural Convective Boundary-Layer Flow of A Nanofluid Past A Vertical Porous Plate Through A Porous Medium. J. of Mod. Meth. in Numer. Math.* 3(1)53–63
- [10] F.A. Soomro, M. Usman, R.U. Haq, W. Wang (2018). Melting heat transfer analysis of Sisko fluid over a moving surface with nonlinear thermal radiation via Collocation method, *Int. J. Heat Mass Tran* 126 1034- 1042.
- [11] Hazem Ali Attia (2015). The Effect of Suction and Injection on the Unsteady Flow Between Two Parallel Plates with Variable Properties *Tamkang J. of Sci. and Eng., Vol. 8(1)* 17- 22
- [12] M. Ijaz, M. Ayub, M.Y. Malik, H. Khan, A.A. Alderremy, S. Aly (2020). Entropy analysis in nonlinearly convective flow of the Sisko model in the presence of Joule heating and activation energy: the Buongiorno model, *Phys. Scripta* 95 (2) 025402
- [13] M. Macha, C.S. Reddy, N. Kishan (2017). Magnetohydrodynamic flow and heat transfer to Sisko nanofluid over a wedge, *Int. J. Fluid Mech. Res.* 44 (1) 1- 13
- [14] M.R. Eid, K.L. Mahny (2018). Flow and heat transfer in a porous medium saturated with a Sisko nanofluid over a nonlinearly stretching sheet with heat generation/absorption, *Heat Tran. Asian Res.* 47 (1) 54- 71.
- [15] M. Jawad, Z. Shah, S. Islam, W. Khan, A.Z. Khan (2019). Nanofluid thin film flow of Sisko fluid and variable heat transfer over an unsteady stretching surface with external magnetic field, *J. Algorithm Comput. Technol.* 13 1e16.
- [16] M. Awais, M.Y. Malik, S. Bilal, T. Salahuddin, Arif Hussain (2017). Magnetohydrodynamic

- (MHD) flow of Sisko fluid near the axisymmetric stagnation point towards a stretching cylinder, *Results Phys.* 7 49e56.
- [17] M. Ali, W.A. Khan, F. Sultan, M. Shahzad (2020). Numerical investigation on thermally radiative time-dependent Sisko nanofluid flow for curved surface, *Phys. Stat. Mech. Appl.* 550 124012
- [18] S.U.S. Choi (1995). Enhancing thermal conductivity of fluids with nanoparticles, *Develop Appl. Non-New Flows* 231 99e105.
- [19] T. Hayat, F. Masood, S. Qayyum, A. Al- saedi (2019). Entropy generation minimization: nonlinear mixed convective flow of Sisko nanofluid, *Pramana* 93 (6), <https://doi.org/10.1007/s12043-019-1838-8>.
- [20] Wubshet Ibrahim, Bandari Shankar (2013). MHD boundary layer flow and heat transfer of a nanofluid, past a permeable stretching sheet with velocity, thermal and solutal slip boundary conditions *Computers & Fluids* (75) 1–10
- [21] Y.S. Daniel, Z.A. Aziz, Z. Ismail, F. Salah (2018). Impact of thermal radiation on electrical MHD flow of nanofluid over nonlinear stretching sheet with variable thickness, *Alexandria Eng. J.* 57 2187